J Appl Electrochem (2009) 39:827–835
DOI 10.1007/s10800-008-9729-6

ORIGINAL PAPER

Electrochemical redox reactions of chromium and iron ions in molten NaCl–2CsCl eutectic for pyro-reprocessing of nuclear fuels

A. Uehara · O. Shirai · T. Nagai · T. Fujii · H. Yamana

Received: 28 June 2008 / Accepted: 14 November 2008 / Published online: 2 December 2008

Abstract Basic electrochemical and spectroscopic properties of Cr^{3+}, Cr^{2+}, Fe^{3+}, and Fe^{2+} were studied to analyze the cyclic redox reactions of Cr and Fe, which may decrease the current efficiency of the electro-winning method using NaCl–2CsCl melts. The formal redox potentials of the $Cr^{3+}|Cr^{2+}$ and $Fe^{3+}|Fe^{2+}$ couples, $E^{\circ\prime}_{Cr^{3+}|Cr^{2+}}$ and $E^{\circ\prime}_{Fe^{3+}|Fe^{2+}}$, in NaCl–2CsCl melts at 923 K were spectroelectrochemically determined to be -0.648 ± 0.005 V and -0.140 ± 0.010 V vs. $Cl_2|Cl^-$, respectively. These values were determined by measuring electromotive force and UV–VIS absorption spectra at varying concentration ratios of trivalent and divalent ions. Cyclic voltammetry was also carried out to examine the characteristics of the voltammograms for the $Cr^{3+}|Cr^{2+}$ and $Fe^{3+}|Fe^{2+}$ couples in NaCl–2CsCl melts. The $E^{\circ\prime}_{Cr^{3+}|Cr^{2+}}$ determined by the spectroelectrochemical method was close to that determined by cyclic voltammetry (-0.651 ± 0.006 V vs. $Cl_2|Cl^-$). The effect of temperature on the $E^{\circ\prime}_{Cr^{3+}|Cr^{2+}}$ in NaCl–2CsCl melts was studied by cyclic voltammetry in the range from 823 to 1,023 K ($E^{\circ\prime}_{Cr^{3+}|Cr^{2+}} = 0.00143T - 1.971 \pm 0.005$ V vs. $Cl_2|Cl^-$). Diffusion coefficients of Cr^{3+} and Cr^{2+}, $D_{Cr^{3+}}$ and $D_{Cr^{2+}}$, were determined between 823 and 1,023 K to be $D_{Cr^{3+}} = 2.23 \times 10^{-3} \exp(-4{,}135/T)$ and $D_{Cr^{2+}} = 3.34 \times 10^{-3} \exp(-4{,}106/T)$, respectively. Molar absorptivities of Cr^{3+} and Cr^{2+} in NaCl–2CsCl melts at 923 K were determined to be 77.8 ± 2.4 M^{-1} cm^{-1} at 17,670 cm^{-1} and 48.0 ± 1.4 M^{-1} cm^{-1} at 9,170 cm^{-1}, respectively. In addition, the effects of these ions on the cyclic redox reaction of the pyro-reprocessing process were discussed.

Keywords NaCl–2CsCl · Cr · Fe · Spectroelectrochemistry · Cyclic redox reaction · Formal redox potential

1 Introduction

The oxide-winning method has attracted technological attention for the pyro-reprocessing of spent oxide fuels of fast breeder reactors [1]. This technique was developed by the Research Institute of Atomic Reactor in Russia, and is considered to have a potential merit as a simplified reprocessing method with good proliferation resistance. This technique is characterized by the electrolytic co-deposition of PuO_2 and UO_2 as a MOX granule from dissolved spent fuels in NaCl–2CsCl melts [1]. In this system, the chemical behavior of the solutes is controlled by the redox condition of the system by electrochemical operation under gas supply of Cl_2 and O_2.

With regard to the current efficiency of this system, it has been reported that the electrolysis efficiency is seriously affected by the cyclic redox reaction of particular co-existing elements. The cyclic redox reaction means an oxidation-reduction reaction between two valence states of the same element, which is supported by the back-and-forth transportation of oxidized and reduced states between anode and cathode.

A. Uehara (✉) · T. Fujii · H. Yamana
Division of Nuclear Engineering Science, Research Reactor Institute, Kyoto University, Kumatori, Osaka 590-0494, Japan
e-mail: auehara@rri.kyoto-u.ac.jp

O. Shirai
Division of Applied Life Science, Graduate School of Agriculture, Kyoto University, Sakyo, Kyoto 606-8502, Japan

T. Nagai
Nuclear Fuel Cycle Engineering Laboratories, Japan Atomic Energy Agency, Tokai, Ibaraki 319-1194, Japan

In this system, because cathode and anode are installed in a crucible without isolation of anode and cathode area, the cyclic redox reaction can easily occur, and this may lead to an extensive reduction in current efficiency. Cr and Fe are particularly considered to cause serious efficiency loss through the cyclic redox reactions between their divalent and trivalent states [2], because they are supplied from the fuel cladding or structural materials. Since the redox potentials of the $Cr^{3+}|Cr^{2+}$ and $Fe^{3+}|Fe^{2+}$ couples are close to that of the $UO_2^{2+}|UO_2$ couple, they are likely to be reduced to divalent states at the cathode for UO_2 deposition. Their divalent states easily move to the anode area by convection, and they are electrochemically re-oxidized at the anode or by reaction with chlorine gas evolved from the anode.

To minimise efficiency loss by the cyclic redox reaction of Cr and Fe, a fundamental understanding on the redox properties of Cr and Fe ions in NaCl–2CsCl melts is important. There have been some published studies of the electrochemical properties of Cr ions in the context of Cr refining. Electrochemically determined redox potentials of the $Cr^{3+}|Cr^{2+}$ couple in LiCl–KCl [3–5], NaCl–KCl [6, 7] and $CaCl_2$–NaCl melts [7, 8] were reported. Smirnov et al. [9] determined the formal redox potential of the $Cr^{3+}|Cr^{2+}$ couple, $E^{o\prime}_{Cr^{3+}|Cr^{2+}}$, by the spectroelectrochemical method in various alkaline metal chlorides. They found that the $E^{o\prime}_{Cr^{3+}|Cr^{2+}}$ shifts negatively depending on the radius of the alkaline metal ions, and this was also found for the $Ni^{3+}|Ni^{2+}$ couple. Some electrochemical studies have been reported for the redox of the $Fe^{3+}|Fe^{2+}$ couple, $E^{o\prime}_{Fe^{3+}|Fe^{2+}}$, in molten chloride, such as eutectic LiCl–KCl [10, 11] and $ZnCl_2$–2NaCl [12]. Most authors have found that the redox reaction of the $Fe^{3+}|Fe^{2+}$ couple is reversible and controlled by the mass transfer of Fe ions to the electrode. However, there have been no reports about the redox reactions of Cr and Fe ions in NaCl–2CsCl melts.

In the above context, this study aims to provide reliable values of $E^{o\prime}_{Cr^{3+}|Cr^{2+}}$ and $E^{o\prime}_{Fe^{3+}|Fe^{2+}}$ in NaCl–2CsCl melts. For this purpose, cyclic voltammetry was adopted and electromotive force measurement with spectrophotometry was also adopted as a complementary technique to determine the precise formal potential. The combination of electrochemical and spectrophotometric measurement has been successfully adopted to the analysis of f-elements by the authors [13–15]. In this technique, which is called spectroelectrochemical technique, the valence is controlled by electrolytic operation and the absorption spectrum and the electromotive force are simultaneously measured.

In addition to the formal redox potentials, their diffusion coefficients and the basic absorption characteristics in NaCl–2CsCl were also reported. On the basis of the experimental results, the possibility of the cyclic redox reactions of Cr and Fe ions in NaCl–2CsCl is discussed.

2 Experimental

2.1 Chemicals

Anhydrous NaCl–2CsCl eutectic (99.99%), $CrCl_3$ (99.99%) and $FeCl_2$ (99.99%) were purchased from Aldrich-APL LLC and used without further treatment. $FeCl_2$ was used for the study of the $Fe^{2+}|Fe^{3+}$ couple to avoid the possible loss of the added sample due to the volatility of $FeCl_3$ even at low temperature (590 K).

2.2 Apparatus

For the spectrophotometric and voltammetric measurements, a three-electrode system with a quartz cell was used. This cell system is designed to perform electrochemical and spectrophotometric measurements simultaneously [13]. A self-registering spectrophotometer V-350 (JASCO Co.) was used for the measurements over wavenumbers from 5,000 to 25,000 cm^{-1}. A pyro-graphite coated graphite rod (Toyo Tanso Co. Ltd.) 3 mm in diameter was used as a working electrode and a silver|silver ion ($Ag|Ag^+$) electrode was used as a reference electrode. This reference electrode consisted of a closed end tube of Pyrex, in which NaCl–2CsCl eutectic containing 4.85 mol% AgCl was put in with a Ag wire of 1 mm diameter. For every experiment, a counter electrode of the same configuration as the reference electrode was used. This was to insulate the anode reaction from the bulk by the Pyrex membrane.

The cell temperature was controlled to the desired temperature in the range 823–1,123 K. An electrochemical measurement system, Hz-3000 (Hokuto Denko Co. Ltd.) was used for the cyclic voltammetry and controlled potential electrolysis [13, 14]. All the experiments were carried out in a glove box filled with a dry argon atmosphere of which the humidity and oxygen impurity was continuously kept less than 1 ppm. In order to compare with various reported values, the potentials measured using 4.85 mol% AgCl in NaCl–2CsCl was converted to that referred to the $Cl_2|Cl^-$ electrode [16].

2.3 Measurement procedures

Cyclic voltammograms were recorded for the redox of Cr^{3+}, Cr^{2+}, and Fe^{2+} at several temperatures. Before starting the measurement, the effect of the potential scanning rate and concentration was initially examined, and the applicable measurement condition was confirmed.

Before the spectroelectrochemical measurement, absorption spectra of pure Cr^{3+}, Cr^{2+}, and Fe^{2+} were measured to determine the molar absorptivities of major absorption bands. After dissolving weighed amount of $CrCl_3$ and $FeCl_2$ into the melts, and confirming the stability

of Cr^{3+} and Fe^{2+} at their equilibrium potential, their spectra were measured. For Cr^{2+}, the spectrum was measured after performing quantitative electro-reduction of initially dissolved Cr^{3+} to Cr^{2+}.

For the spectroelectrochemical measurement on $E^{\circ\prime}_{Cr^{3+}|Cr^{2+}}$ in NaCl–2CsCl melts, stepwise electrolytic reduction was repeated. At each step, a portion of Cr^{3+} was reduced to Cr^{2+} by controlled potential electrolysis for about 600 s. During this time the absorption spectrum and equilibrium potential, which is the electromotive force between the working and reference electrode, were measured. This step was repeated until the reduction of Cr^{3+} to Cr^{2+} was completed. For the case of $E^{\circ\prime}_{Fe^{3+}|Fe^{2+}}$ in NaCl–2CsCl melts, stepwise oxidation of Fe^{2+} to Fe^{3+} followed by absorption measurement was repeated.

The concentrations of Cr^{3+} and Cr^{2+} were determined from the intensity of their characteristic absorption bands. Because Fe^{3+} has no distinct absorption band, Fe^{3+} concentration was estimated by subtracting the Fe^{2+} concentration, which was determined by absorptiometry, from the total concentration of Fe. The natural logarithms of the concentration ratio of $Cr^{3+}|Cr^{2+}$ and $Fe^{3+}|Fe^{2+}$ were plotted as a function of the equilibrium potential, and $E^{\circ\prime}_{Cr^{3+}|Cr^{2+}}$ or $E^{\circ\prime}_{Fe^{3+}|Fe^{2+}}$ were determined on the base of the Nernst equation.

3 Results and discussion

3.1 Redox reaction and absorption spectra of Cr ions in NaCl–2CsCl melts

3.1.1 *Electrochemical properties of the* $Cr^{3+}|Cr^{2+}$ *couple*

Figure 1 shows the voltammograms of NaCl–2CsCl melts containing 0.0151 M $CrCl_3$, recorded at 923 K using a pyro-graphite carbon working electrode. Cathodic and anodic peak currents were observed, and these were attributed to the redox reaction of the $Cr^{3+}|Cr^{2+}$ couple. It was found that peak currents were proportional to the square root of potential scanning rate in the range from 0.05 to 0.5 Vs^{-1}. It was also found that peak currents were proportional to the concentration of Cr^{3+} in the concentration range from 0.0151 to 0.147 M (M = mol dm^{-3}). It was concluded that the redox reaction of the $Cr^{3+}|Cr^{2+}$ couple is reversible and controlled by diffusion under the applied conditions.

Potential differences between cathodic and anodic peaks was found to be independent of the potential scanning rate and constant to be 0.195 ± 0.010 V over the range from 0.05 to 0.5 V s^{-1}. This indicates that the redox reaction of the $Cr^{3+}|Cr^{2+}$ couple is a reversible reaction of one-electron exchange. The mid-point potential of the cathodic and anodic peaks, $E_{1/2,Cr^{3+}|Cr^{2+}}$, was -0.665 ± 0.003 V vs. $Cl_2|Cl^-$.

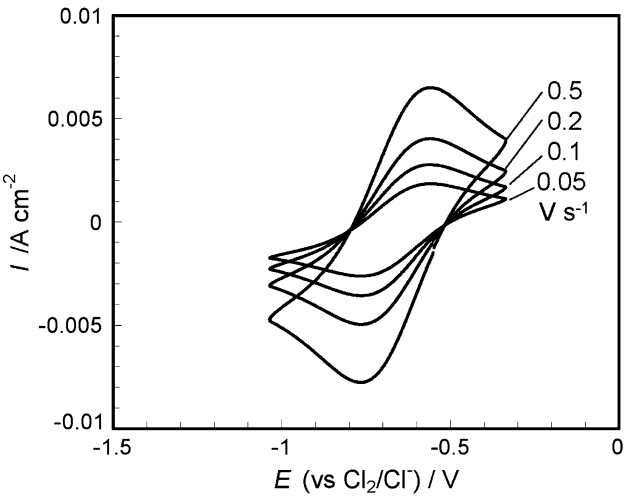

Fig. 1 Cyclic voltammogram for the redox reaction of the Cr^{3+}/Cr^{2+} couple in molten NaCl–2CsCl at 923 K recorded at the potential scanning rate between 0.5 and 0.05 V s^{-1}. Working electrode: pyro-graphite carbon electrode. Concentration of $CrCl_3$: 0.0151 M

The $E^{\circ\prime}_{Cr^{3+}|Cr^{2+}}$ is expressed by the following equation;

$$E_{1/2,Cr^{3+}|Cr^{2+}} = E^{\circ\prime}_{Cr^{3+}|Cr^{2+}} + (RT/F)\ln\left(D_{Cr^{3+}}/D_{Cr^{2+}}\right)^{1/2} \quad (1)$$

where R, T, F, $D_{Cr^{3+}}$ and $D_{Cr^{2+}}$ are gas constant, absolute temperature, Faraday constant, diffusion coefficients of Cr^{3+} and Cr^{2+}, respectively. The $D_{Cr^{3+}}$ and $D_{Cr^{2+}}$ were obtained by the following equation [17];

$$I_p = 0.4463F^{3/2}A(RT)^{-1/2}D^{1/2}cv^{1/2} \quad (2)$$

where I_p, A, c and v were peak current, electrode surface area, concentration and potential scanning rate, respectively. The $D_{Cr^{3+}}$ at 923 K was calculated to be 2.50×10^{-5} cm^2 s^{-1}. In order to determine $D_{Cr^{2+}}$, Cr^{3+} was quantitatively reduced to Cr^{2+} by controlled potential electrolysis and cyclic voltammetry was performed. $D_{Cr^{2+}}$ at 923 K was calculated to be 3.85×10^{-5} cm^2 s^{-1}. Cyclic voltammograms for the redox reaction of the $Cr^{3+}|Cr^{2+}$ couple were carried out at temperatures between 823 and 1,023 K, $E_{1/2,Cr^{3+}|Cr^{2+}}$, $D_{Cr^{3+}}$ and $D_{Cr^{2+}}$ were determined. $E^{\circ\prime}_{Cr^{3+}|Cr^{2+}}$ was obtained at temperatures between 823 and 923 K as shown by Eq. 3.

$$E^{\circ\prime}_{Cr^{3+}|Cr^{2+}} = 0.00143T - 1.971 \pm 0.005(\text{V vs. } Cl_2|Cl^-) \quad (3)$$

In Table 1, results for $E^{\circ\prime}_{Cr^{3+}|Cr^{2+}}$ in NaCl–2CsCl are compared to other reported values in various chloride melts. The temperature dependency of the NaCl–2CsCl system is larger than those in other molten chlorides, such as LiCl–KCl, NaCl, KCl, CsCl, NaCl–KCl, NaCl–CsCl and KCl–CsCl, [7, 9]. This tendency of NaCl–2CsCl melts is

Table 1 Formal redox potential of the Cr^{3+}/Cr^{2+} couple, $E^{\circ\prime}_{Cr^{3+}|Cr^{2+}}$, in various molten salts

Melt	$E^{\circ\prime}_{Cr^{3+}\|Cr^{2+}}$	T (K)	$E^{\circ\prime}_{Cr^{3+}\|Cr^{2+}}$ at 823 K/V	References
NaCl–2CsCl	0.00143T–1.971	823–1,023	− 0.794	This study
LiCl–KCl	0.00115T–1.679	643–823	− 0.7326	[3]
NaCl	0.001120T–1.627	1,073–1,173	(−0.705)	[7]
KCl	0.000550T–1.167	1,073–1,173	(−0.714)	[7]
CsCl	0.000320T–1.028	1,073–1,173	(−0.765)	[7]
NaCl–KCl	0.00100T–1.575	1,073–1,173	(−0.752)	[7]
NaCl–CsCl	0.000800T–1.397	1,073–1,173	(−0.739)	[7]
KCl-CsCl	0.000550T–1.228	1,073–1,173	(−0.775)	[7]
NaCl–KCl	0.001173T–1.817	993–1,233	(−0.852)	[9]

common for $U^{4+}|U^{3+}$ and $Eu^{3+}|Eu^{2+}$ couples in chloride melts [14, 15]. This means that the standard entropy change of the chloride complexes of these ions in NaCl–2CsCl melts is larger than those in other chloride melts, suggesting that the structure of their chloride complexes in NaCl–2CsCl melts has unique characteristics.

At 923 K, the redox potential of the $UO_2^{2+}|UO_2$ couple is −0.65 V vs. $Cl_2|Cl^-$ [1, 2], which is close to the value for $E^{\circ\prime}_{Cr^{3+}|Cr^{2+}}$. Therefore, the reduction of Cr^{3+} ions in molten NaCl–2CsCl easily occurs at the cathode, whose potential is controlled to about −0.65 V vs. $Cl_2|Cl^-$ for UO_2 deposition.

Diffusion coefficients, D, of Cr^{3+} and Cr^{2+}, were formulated as an Arrhenius equation as follows;

$$D = D^{\circ} \exp(-E_a/RT) \quad (4)$$

where D° and E_a are frequency factor and activation energy, respectively. In Fig. 2, ln D of Cr ions are plotted versus the inverse of the temperature, by which D° and E_a were obtained. In Table 2 values of $D_{Cr^{3+}}$ and $D_{Cr^{2+}}$ in NaCl–2CsCl are shown and compared with literature values for other chloride melts. The apparent activation energies for Cr^{3+} and Cr^{2+} in NaCl–2CsCl were calculated to be 34.4 and 34.1 kJ mol^{-1}, respectively.

At 823 K, $D_{Cr^{3+}}$ in NaCl–2CsCl is close to that in LiCl–KCl [3], but $D_{Cr^{2+}}$ in NaCl–2CsCl is smaller than that in LiCl–KCl. In other words, $D_{Cr^{2+}}$ is 1.6 times higher than $D_{Cr^{3+}}$ in NaCl–2CsCl, and this is not the case for the LiCl–KCl system. It should be noted that the activation energies of Cr^{3+} and Cr^{2+} in NaCl–2CsCl are smaller than those of the LiCl–KCl system, but that D° are larger in NaCl–2CsCl than in LiCl–KCl. This is a characteristic of NaCl–2CsCl melts.

Generally, the chloride complexes of Cr^{3+} and Cr^{2+} in molten chloride are considered to be $CrCl_6^{3-}$ (octahedral) and $CrCl_4^{2-}$ (tetrahedral), respectively [18], and D of metal ions decreases with increasing radius of the alkali metal ion [19] owing to the decrease in the counter polarizing effect of Li to Cs. These differences of the complex structure, as well as of the difference in the interaction with Cl^-, may give the characteristics of their diffusion coefficients in a melt that is rich in CsCl.

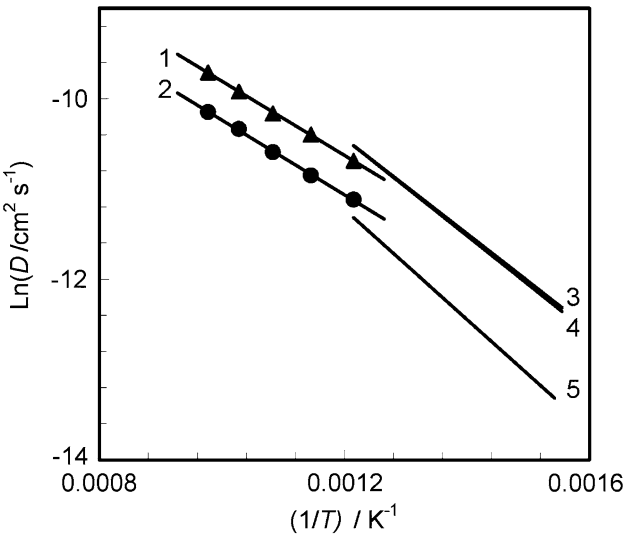

Fig. 2 The diffusion coefficients of Cr^{3+} and Cr^{2+} depended on the temperature determined based on the cyclic voltammogram. Lines 1 and 2; $D_{Cr^{2+}}$ and $D_{Cr^{3+}}$ in NaCl–2CsCl, lines 3 and 4; $D_{Cr^{2+}}$ and $D_{Cr^{3+}}$ in LiCl–KCl [3], line 5; $D_{Cr^{3+}}$ in LiCl–KCl [5], respectively

3.1.2 *Absorption spectra of Cr^{3+} and Cr^{2+} and spectroelectrochemical determination of the formal redox potential*

Figure 3 shows the absorption spectrum of Cr^{3+} in NaCl–2CsCl at 923 K. The color of Cr^{3+} in NaCl–2CsCl molten salt was purple, and it shows two distinct absorption bands at 17,670 cm^{-1} (566 nm) and 11,990 cm^{-1} (834 nm). The absorption intensity at 17,670 cm^{-1} was found to be proportional to the concentration, in the range 2.57×10^{-3}–1.14×10^{-2} M. The molar absorptivity of the bands at 17,670 cm^{-1} and 11,880 cm^{-1} were 77.8 ± 2.4 and 52.0 ± 1.6, respectively. This spectrum of Cr^{3+} in NaCl–2CsCl is

Table 2 Diffusion coefficients of Cr^{3+} and Cr^{2+}, $D_{Cr^{3+}}$ and $D_{Cr^{2+}}$, respectively, in various molten salts

Melt	$D_{Cr^{3+}}, D_{Cr^{2+}}$ ($cm^2\ s^{-1}$)	T (K)	D at 823 K/$cm^2\ s^{-1}$	References
NaCl–2CsCl	$D_{Cr^{3+}} = 2.23 \times 10^{-3} \exp(-4,135/T)$	823–1,023	1.46×10^{-5}	This study
NaCl–2CsCl	$D_{Cr^{2+}} = 3.34 \times 10^{-3} \exp(-4,106/T)$	823–1,023	2.28×10^{-5}	This study
LiCl–KCl	$D_{Cr^{3+}} = 1.87 \times 10^{-2} \exp(-5,386/T)$	643–823	2.70×10^{-5}	[3]
LiCl–KCl	$D_{Cr^{2+}} = 1.64 \times 10^{-2} \exp(-5,276/T)$	643–823	2.69×10^{-5}	[3]
LiCl–KCl	$D_{Cr^{3+}} = 1.95 \times 10^{-2} \exp(-6,077/T)$	648–823	1.21×10^{-5}	[5]
$CaCl_2$–NaCl	$D_{Cr^{3+}}, D_{Cr^{2+}}$	823	1.0×10^{-5}	[8]

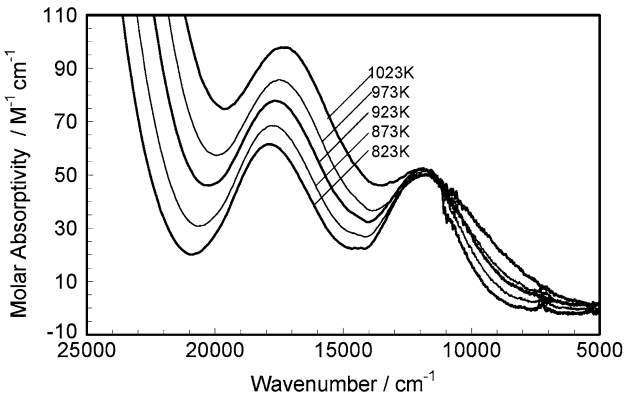

Fig. 3 Absorption spectra of Cr^{3+} at various temperatures in molten NaCl–2CsCl. Temperature: 823, 873, 923, 973 and 1,023 K, respectively

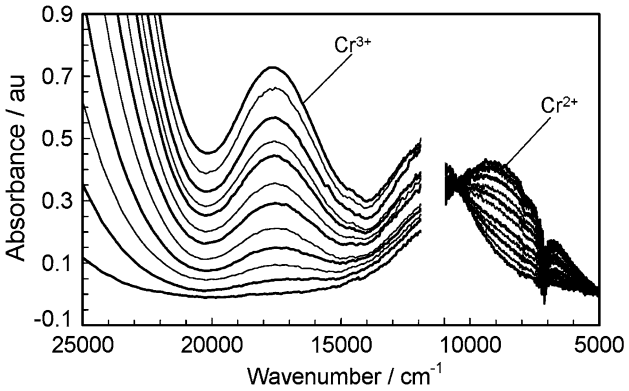

Fig. 4 Absorption spectra after the controlled potential difference electrolysis for the reduction of Cr^{3+} in molten NaCl–2CsCl at 923 K. Concentration of $CrCl_3$: 8.94×10^{-3} M

similar to that in LiCl–KCl, but there is slight difference in the peak energy and absorption intensity.

There is some literature which describes the absorption spectrum of Cr^{3+} in molten LiCl–KCl [17, 20]. According to Gruen [18], in LiCl–KCl melts, two broad bands at 18,500 and 12,500 cm^{-1} are observed, and these are attributable to the presence of $CrCl_6^{3-}$. These bands were assigned to transitions of $^4A_2 \rightarrow {}^4T_1(^4F)$ and $^4A_2 \rightarrow {}^4T_2(^4F)$, respectively. Absorption bands at 17,670 and 11,990 cm^{-1} observed in this study correspond to these two transitions, even though the peak energies are slightly different to the LiCl–KCl system. The slightly smaller transition energy of the peaks in NaCl–2CsCl are presumably attributable to the slight difference in the complex status of $CrCl_6^{3-}$ in a CsCl-rich melt, in which the octahedral structure of the metal complex is likely to have more symmetry. Temperature dependence of the absorption spectrum was studied as shown in Fig. 3. The absorption peak at 18,180 cm^{-1} was found to shift toward the lower energy side with increasing temperature from 823 to 1,023 K, while the peak energy of absorption at 11,990 cm^{-1} was independent of temperature. On the other hand, the absorption region between 11,000 and 6,000, which is the shoulder part of the peak of 11,990 cm^{-1}, was found to increase slightly with increasing temperature. These observations are similar to those of the spectrum of Cr^{3+} in the LiCl–KCl system [18].

In order to observe the absorption spectra of Cr^{2+}, reductive controlled potential electrolysis was carried out. Constant potential $(-0.9\ \text{to}\ -1.2\ \text{V vs. } Cl_2|Cl^-)$ was applied for 500–5,000 s, and the change of the spectrum was observed. As the electrolysis proceeded, a prominent absorption band at 9,170 cm^{-1} (1,090 nm) was found to grow, while the two absorption bands of Cr^{3+} gradually decreased. An isosbestic point was observed at 10,530 cm^{-1} and the molar absorptivity of this point was 38 ± 1.2. When the electrolysis was completed, the absorption intensity at 17,670 cm^{-1} became almost zero. This confirmed the complete reduction of Cr^{3+} to Cr^{2+}. The molar absorptivity of the peak absorption by Cr^{2+} at 9,170 cm^{-1} was found to be 48.0 ± 1.4. This single absorption peak is quite similar to the spectrum of Cr^{2+} observed in the LiCl–KCl system [18]. The change in the spectrum during the electrolysis is shown in Fig. 4.

The electrolytic reduction of Cr^{3+} was performed in a stepwise fashion to change the ratio of Cr^{3+} and Cr^{2+}. At each step of the reduction, immediately after the completion of the electrolytic operation for about 600 s, the spectrum and the electromotive force between the working and reference electrode was recorded. The concentration of Cr^{3+} and Cr^{2+} at each step were calculated from the absorbance at 17,670 and 9,170 cm^{-1} with their molar absorptivities.

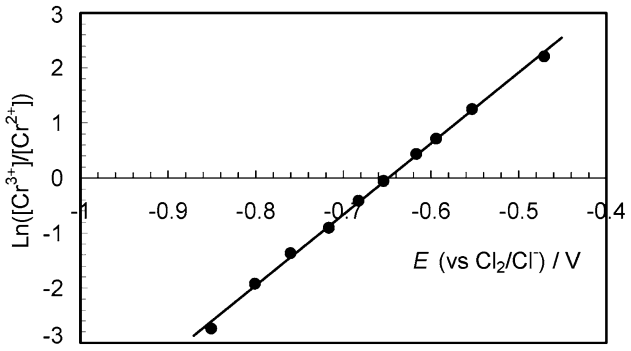

Fig. 5 Relation between the natural logarithm of the ratio of the concentration of Cr^{3+} to that of Cr^{2+}, $\ln([Cr^{3+}]/[Cr^{2+}])$, and the equilibrium potential in molten NaCl–2CsCl at 923 K

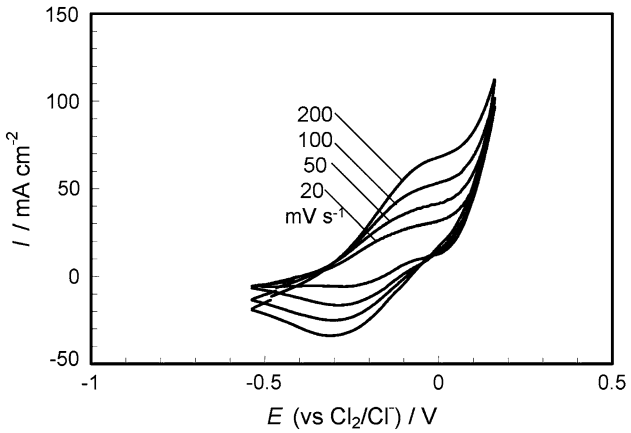

Fig. 6 Cyclic voltammogram of Fe in NaCl–2CsCl melts at 923 K recorded at the potential scanning rate between 0.2 and 0.02 V s^{-1}. Working electrode: pyro-graphite carbon electrode. The concentration of $FeCl_2$: 0.119 M

The natural logarithm of the concentration ratio of Cr^{3+} to that of Cr^{2+} at each step was plotted as a function of the equilibrium potential as shown in Fig. 5. $E^{\circ\prime}_{Cr^{3+}|Cr^{2+}}$ is given by the potential where the concentrations of Cr^{3+} and Cr^{2+} become equal, namely the potential at the intersection of the plotted line and the *x*-axis. The slope of the line was 12.9, which is close to theoretical value for a one electron redox reaction, 12.6. As a result, $E^{\circ\prime}_{Cr^{3+}|Cr^{2+}}$ at 923 K was determined to be -0.648 ± 0.005 V vs. $Cl_2|Cl^-$. This agrees very well with $E^{\circ\prime}_{Cr^{3+}|Cr^{2+}}$ obtained by cyclic voltammetry, -0.651 ± 0.006 V vs. $Cl_2|Cl^-$. This agreement demonstrates the adequacy and reliability of the voltammetric determination of $E^{\circ\prime}_{Cr^{3+}|Cr^{2+}}$.

3.2 Redox reaction and absorption spectra of Fe ion in NaCl–2CsCl melts

3.2.1 Electrochemical properties of the $Fe^{3+}|Fe^{2+}$ *couple*

Figure 6 shows the cyclic voltammogram of $FeCl_2$ in NaCl–2CsCl at 923 K. Because of the presence of the redox reaction of the $Cl_2|Cl^-$ couple, the cyclic voltammogram seems to rise toward the positive potential side. The cathodic peak of the reduction of Fe^{3+} to Fe^{2+} is seen at -0.29 V vs. $Cl_2|Cl^-$. However the peak maximum of the anodic current is difficult to decide due to the rising background current by chlorine gas evolution. In order to make the peak finding clearer, the background current of Cl_2 evolution was initially measured with blank melt and subtracted from the anodic current of Fe^{2+}. As a result, the mid-point potential of the anodic and cathodic peaks of the $Fe^{3+}|Fe^{2+}$ couple, $E_{1/2,Fe^{3+}|Fe^{2+}}$, was determined to be -0.177 ± 0.020 V vs. $Cl_2|Cl^-$ at 923 K.

In this voltammetric process there were several indications that the redox reaction of $Fe^{3+}|Fe^{2+}$ cannot be analyzed ideally. The cathodic peak potential was found to shift negatively with increasing scanning rate, which is a sign of irreversibility of the reaction. There are other disturbing reactions that make electrochemical analysis difficult, such as oxidation of Fe^{2+} by Cl_2 by reactions (5) and (6) and vaporization of $FeCl_3$.

$$2Cl^- \rightarrow Cl_2 + 2e^- \quad (5)$$

$$FeCl_2 + 1/2Cl_2 \rightarrow FeCl_3 \uparrow \quad (6)$$

It was concluded that $E^{\circ\prime}_{Fe^{3+}|Fe^{2+}}$ cannot be determined precisely by cyclic voltammetry.

3.2.2 Absorption spectra of Fe^{2+} *and spectroelectrochemical determination of the formal redox potential*

Absorption spectra were measured at 923 K in NaCl–2CsCl containing 6.56×10^{-3} M $FeCl_2$. The result is shown in Fig. 7a in which a broad absorption band at 5,840 cm^{-1} is characteristic. When the concentration of Fe^{2+} in the melts was increased, it was found that the absorption band shifts to the higher wave number side and that the increase in the absorption intensity is not proportional to the concentration increase. The correlation between the absorption intensity of the peak maximum and the concentration of Fe^{2+} is shown in Fig. 7b, in which a non-linear relation is clearly seen. We have no clear explanation of this unique effect, but can point out the possible influence of Fe^{2+}–Fe^{2+} interaction, or change in the melt structure with increasing Fe^{2+} concentration. Even though there was no clear explanation of this effect we concluded that, by using the non-linear calibration curve of Fig. 7b, estimation of the Fe^{2+} concentration from observed absorption intensity is possible.

The temperature dependence of the absorption spectrum of Fe^{2+} was studied in the temperature range 823 to 1,023 K. As shown in Fig. 8, with increasing temperature, the main absorption band split into two prominent peaks

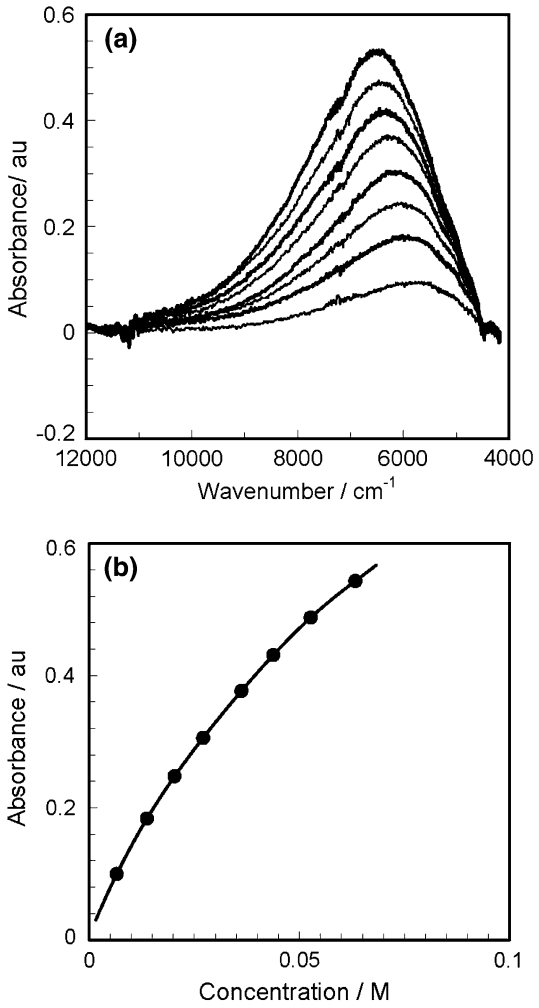

Fig. 7 **a** Absorption spectra of Fe^{2+} of various concentrations in NaCl–2CsCl melts at 923 K. **b** The relation between concentration of Fe^{2+} and peak intensity

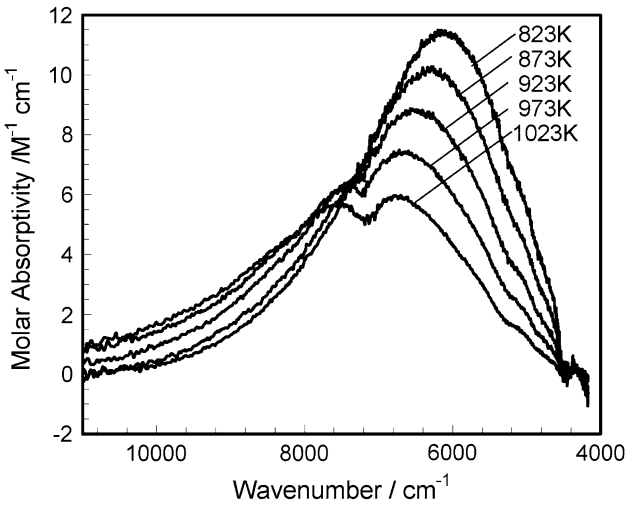

Fig. 8 Absorption spectra of Fe^{2+} in NaCl–2CsCl melt at various temperatures between 823 and 1,023 K

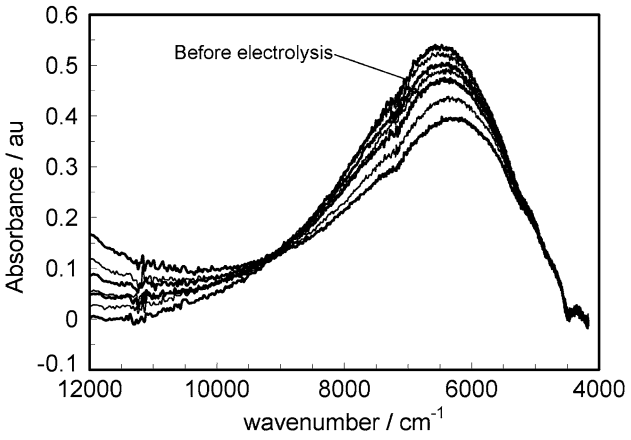

Fig. 9 Absorption spectra after the controlled potential difference electrolysis for the oxidation of Fe^{2+} in NaCl–2CsCl melt at 923 K. The concentration of $FeCl_2$; 6.33×10^{-2} M

and their peak positions blue-shifted. The major peak loses its intensity, with increase in temperature, which is similar for the LiCl–KCl system [20]. This transition is assigned to $FeCl_4^{2-}$ in the melts, and the observed temperature effect may be due to the change in structural symmetry of the tetrahedral complex, or to the increasing ionicity of the Fe–Cl bond, which is analogous to the case of $CoCl_4^{2-}$ [20].

In order to determine $E^{\circ\prime}_{Fe^{3+}|Fe^{2+}}$, spectroelectrochemical technique was adopted at 923 K. Oxidation of Fe^{2+} to Fe^{3+} was performed at -0.2 to 0 V vs. $Cl_2|Cl^-$ in a stepwise manner. At each step, the equilibrium potential and absorption spectrum were measured. The stepwise variation of the absorption spectrum along with the progressing oxidation is shown in Fig. 9. The absorption intensity in the IR region gradually decreased, while absorption intensity in the UV region gradually increased. The absorption in the UV region is attributable to Fe^{3+} generated. An isosbestic point was observed at 9,140 cm^{-1}, and this suggests that the redox pair is controlled successfully.

$E^{\circ\prime}_{Fe^{3+}|Fe^{2+}}$ was determined in the same manner as for the $Cr^{3+}|Cr^{2+}$ couple. The concentration of Fe^{2+} was determined using the calibration curve of Fig. 7b. Because Fe^{3+} has no distinct peak maximum in the observed range, its concentration was calculated by subtracting Fe^{2+} concentration from the total concentration of Fe, which was defined from the added amount of the starting material. Here, the loss of $FeCl_3$ by evaporation was neglected because the experimental time was limited.

The natural logarithm of the concentration ratio of Fe^{3+} to that of Fe^{2+} was plotted as a function of equilibrium potential as shown in Fig. 10. In the potential region higher than -0.2 V vs. $Cl_2|Cl^-$, both equilibrium potential measurement and absorption spectrum measurement were disturbed to a great extent. This results from the above mentioned disturbing reactions in this region, and plots in

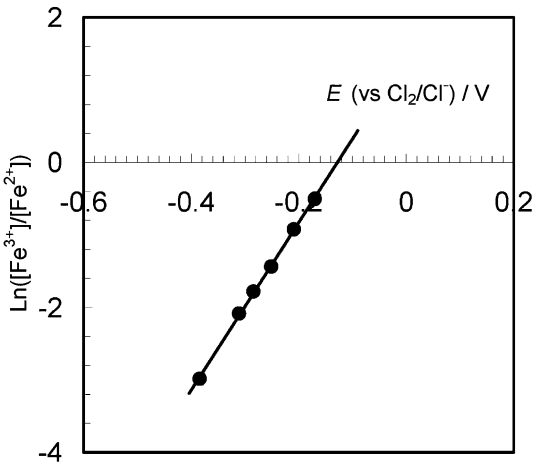

Fig. 10 Relation between the natural logarithm of the concentration ratio of Fe^{3+} to that of Fe^{2+}, $\ln([Fe^{3+}]/[Fe^{2+}])$, and the equilibrium potential in molten NaCl–2CsCl at 923 K

this region were so scattered that they are not shown in the figure. The Nernst linear relation was analyzed in plots of the potential region lower than -0.2 V vs. $Cl_2|Cl^-$. This showed a quite satisfactory linear line, and this was extrapolated to the higher potential region to obtain the intersection point with the *X*-axis.

The slope of this line was 11.5, which agrees well with the theoretical slope for a one electron redox reaction at 923 K, 12.6, which supports the validity of this analysis. As a result, $E^{\circ\prime}_{Fe^{3+}|Fe^{2+}}$ was determined to be -0.127 ± 0.010 V. This is slightly more positive than $E_{1/2,Fe^{3+}|Fe^{2+}}$ by cyclic voltammetry. The determined $E^{\circ\prime}_{Fe^{3+}|Fe^{2+}}$ at 923 K should be a precise and reliable value, which is difficult to determine precisely by the voltammetric technique.

3.3 The cyclic redox reaction of Cr and Fe in the pyro-reprocessing process

Vavilov et al. [1] and Kobayashi et al. [2] investigated the current efficiency of the pyro-process, in terms of the conditions of U, Pu, lanthanides, Fe, Cl_2 gas, and O_2 gas. They suggest that the electrolytic efficiency decreases with increasing concentration of lanthanides and Fe ions, and point out the possibility of cyclic redox reactions.

$E^{\circ\prime}_{Cr^{3+}|Cr^{2+}}$ in NaCl–2CsCl was found to be more negative than that in LiCl–KCl. The cathode potential for the deposition of UO_2 from NaCl–2CsCl is about -0.65 V vs. $Cl_2|Cl^-$, and this is very close to the redox potential of the $Cr^{3+}|Cr^{2+}$ couple. This means that in this melt, the reduction of Cr^{3+} to Cr^{2+} should occur at the cathode together with UO_2 deposition. The potential of the anode under operation is close to zero V vs. $Cl_2|Cl^-$ because oxidation of Cl^- to Cl_2 gas is the major anode reaction, and thus, Cr^{2+}, which migrates from cathode area to anode, is re-oxidized. The repetition of this process certainly leads to the cyclic redox reaction of Cr the ion, and its contribution to loss of current efficiency is more serious with higher concentration of Cr ion in the melts.

In contrast to the case of Cr, $E^{\circ\prime}_{Fe^{3+}|Fe^{2+}}$ in NaCl–2CsCl was determined to be -0.140 ± 0.010 V, which is rather close to the potential of the anode under operation. This means that Fe exists in divalent state in the cathode area. The potential of the anode, which is close to zero V vs. $Cl_2|Cl^-$, has insufficient overpotential for the fast oxidation of Fe^{2+} to Fe^{3+}. However, in the vicinity of the anode, there exists a large amount of Cl_2 gas, which is evolved from the anode, and this promotes oxidation of Fe^{2+} to Fe^{3+} in the bulk. Therefore, the cyclic redox reaction of the Fe ion is also possible in this system. Because $FeCl_3$ has rather high volatility, oxidized Fe^{3+} is likely to evaporate with Cl_2 gas and to be removed to the off-gas system. Fe and Cr alloys are the structural materials of fast breeder fuel bundles and pins and avoidance of fuel structural materials finding their way into the melts would improve the current efficiency markedly.

4 Conclusion

For the analysis of the cyclic redox reactions of Cr and Fe ions, which may accelerate the current efficiency loss of the electro-winning method using NaCl–2CsCl melts, basic electrochemical and spectroscopic properties of Cr^{3+}, Cr^{2+}, Fe^{3+}, and Fe^{2+} were studied. Their absorption spectra were measured, and the molar absorptivities of their characteristic absorption bands were determined. By adopting cyclic voltammetry and spectroelectrochemistry, $E^{\circ\prime}_{Cr^{3+}|Cr^{2+}}$ was precisely determined. $E^{\circ\prime}_{Fe^{3+}|Fe^{2+}}$ was precisely determined the spectroelectrochemical method.

Result for $E^{\circ\prime}_{Cr^{3+}|Cr^{2+}}$ and $E^{\circ\prime}_{Fe^{3+}|Fe^{2+}}$ were within the potential range of the operation condition of fuel reprocessing, and thus the high possibility of cyclic redox reactions of Cr and Fe ions in the process is suggested. Basic spectrophotometric properties of these ions, such as spectrum and molar absorptivities will be beneficial for further analytical work of Cr and Fe ions in NaCl–2CsCl melts.

Acknowledgement We thank Mr. Roy Jacobus for his help in improving the English expressions of this paper.

References

1. Vavilov S, Kobayashi T, Myochin M (2004) J Nucl Sci Technol 41:1018
2. Kobayashi T, Fukushima M, Fujii K (2005) J Nucl Sci Technol 42:861
3. Bemslimane K, Lantelme F, Chemla M (1992) Electrochim Acta 37:1445
4. Inman D, Legey J, Spencer R (1975) J Electroanal Chem 61:289

5. Cotarta A, Bouteillon J, Poignet JC (1997) J Appl Electrochem 27:651
6. Cho K, Kuroda T (1971) Denki Kagaku 39:206
7. Tumidajski PJ, Flengas SN (1991) J Electrochem Soc 138:1659
8. Martinez AM, Castrillejo Y, Borresen B, Bermejo MR, Vega M (2000) J Electroanal Chem 493:1
9. Smirnov MV, Potapov AM (1994) Electrochim Acta 39:143
10. Inman D, Legey JC, Spencer R (1978) J Appl Electrochem 8:269
11. Poignet JC, Barbier MJ (1972) Electrochim Acta 17:1227
12. Castrillejo Y, Martinez AM, Vega M, Barrado E, Picard G (1995) J Electroanal Chem 397:139
13. Nagai T, Fujii T, Shirai O, Yamana H (2004) J Nucl Sci Technol 41:690
14. Nagai T, Uehara A, Fujii T, Shirai O, Sato N, Yamana H (2005) J Nucl Sci Technol 42:1025
15. Uehara A, Shirai O, Nagai T, Fujii T, Yamana H (2007) Z Naturforsch 62:191
16. Shirai O, Nagai T, Uehara A, Yamana H (2008) J Alloys Compd 456:498
17. Bard AJ, Faulkner LR (2001) Electrochemical methods: fundamentals and applications, 2nd edn. Wiley, New York, p 231
18. Gruen DM, McBeth RL (1963) Coordination chemistry. Butterworths, London, pp 23–47
19. Janz GJ, Bansal NP (1982) J Phys Chem Data 11:505
20. Harrington G, Sundheim BR (1960) Ann N Y Acad Sci 79:950